43rd Aerospace Sciences Meeting and Exhibit
9-13 January 2005, Reno, Nevada

AIAA -2005-1032

Distributed Measurement of Aerodynamic Loads Using a Small Scale Wind Tunnel Model

Roy J. Hartfield, Jr. † and John E. Burkhalter‡
Aerospace Engineering, Auburn University, Auburn, AL

Abstract

A method for accurately measuring the drag associated with a protuberance on an aircraft has been devised and implemented in a wind tunnel using a C-130 model. The C-130 aircraft has been heavily modified for various different configurations and the impact that these modifications have had on the aerodynamic performance of the aircraft has not been well documented. This paper describes a methodology for using a relatively small scale (1/48th) model in a wind tunnel to obtain accurate measurements of the aerodynamic drag for various protrusions on the full-scale aircraft.

Measurement Theory and Aerodynamic Scaling

In order to measure the drag associated with each protuberance, one might choose to measure the drag of the aircraft *without* the protuberance and then measure the drag *with* the protuberance using standard wind tunnel techniques[1] and subtract the two measurements to obtain the drag produced by the protuberance. For a 1/48th scale wind tunnel model and a balance with a 25 pound axial force gage, this method for obtaining drag data on a small protuberance results in an effort to measure load differences on the order 0.002 pounds to .015 pounds if one drag count is the required accuracy. Measurements this small are usually buried in measurement uncertainty[2] but in some cases, may be obtained with very limited accuracy.

To accurately and reliably measure the drag contribution of each protuberance, another means of measuring the drag associated with each protuberance is needed. Consequently, drag sensors were designed for each protuberance and these individual load cells were mounted inside the fuselage. Each protuberance was attached to an individual sensor and the drag was measured directly. The sensitivity of each sensor was controlled by the design and resulted in measurements that did ***not*** depend on the difference of two large numbers.

The second substantial practical issue related to accurate measurement of drag on a protuberance in the wind tunnel is the viscous component of the drag. The Reynolds number in the wind tunnel test is quite different from the full scale flight Reynolds number. For the C-130 aircraft, with an air speed of about 250 knots at an altitude of 5000 feet, the full-scale Reynolds number (based on the aircraft reference length) is approximately 3.2×10^7. In a subsonic tunnel, for a given size model, the only practical way to change the Reynolds number is by varying the tunnel speed, V. In the present test for the1/48th

† Associate Professor, Aerospace Engineering, Senior Member AIAA
‡ Professor, Aerospace Engineering, Associate Fellow AIAA

scale model, the Reynolds number is about 2.7 $x10^5$, about two orders of magnitude less than the full size. This large difference in Reynolds number can lead to erroneous results and wrong conclusions as it related to the measurement of drag. This large discrepancy does not mean that large errors are necessarily introduced into the drag measurements, but indeed illustrates that care must be exercised in interpreting drag measurements in a wind tunnel and making direct application to the full scale aircraft.

To exacerbate the problem, the boundary layer thickness as a function of axial distance along the fuselage is proportionally different for the full size aircraft and the wind tunnel model. For the present case, computations were made to estimate the boundary thickness on the full-scale aircraft. At the aft end of the fuselage just in front of the vertical tail, the boundary layer thickness on the full-scale aircraft at full scale Reynolds number is estimated using standard viscous boundary layer theory to be 5.2 inches.[3]

To assess the boundary layer conditions on the model, a pitot-probe based series of measurements were carried out on a “clean” C-130 model. At the same location on the model, the boundary layer is approximately 0.2 in. (5 mm) thick. This is proportionally approximately twice as thick as the full-scale aircraft boundary layer. This information is needed for the design and placement of the protrusions.

To correlate the protuberance size/locations, it is noted that a protuberance on the full-scale aircraft that is 16 inches high is positioned well outside the fuselage boundary layer and “sees” the free stream velocity at that point. While on the model a scaled 16 inch protuberance (16/48) is only .33 inches high and thus is mostly in the model fuselage boundary layer. This means that 1/48th scaled protuberances will not register the same relative loads as the full-scale protuberance.

Two different methods were used to solve this problem and obtain more realistic drag coefficient measurements. For the some protrusions, the boundary layer thickness was used to help size the protuberance. That is, even though the model is a 1/48 scale, it is not necessary that each protuberance be 1/48 scale. Consequently, some protrusions were designed to be 1/32nd scale. These scaled protuberances were thus placed outside the boundary layer in regions where the actual protuberance was outside the boundary layer. For other protuberances, resizing was not feasible because the fairings must approximately fit the model scale in order for the overall flow conditions to be reproduced around the model. In these cases, the protuberances were mounted at a standoff distance from the fuselage appropriate to place the protuberances outside the boundary layer to obtain more accurate drag results.

A third concern relating to the measurement of drag introduced by a particular protuberance involves the interference between the protuberance of interest and the remainder of the aircraft including other protuberances. This interference occurs both on the model and on the full scale aircraft. This interference may be very significant in the case of antennas lined up in a row on the top of a fuselage, for example or the interference may be minimal in the case of a wing-mounted fuel tank for example. For the distributed load measurements, the additional loads placed on surrounding protuberances can be assessed from wind tunnel tests; however, modifications to the aerodynamic loading of the fixed airframe can only be assessed using other methods such as sting-balance load measurements. Fortunately, this particular category of drag inducement is a minor contribution to drag for the

testing results presented in this paper. This is due partly to the absence of protuberances of significant size place in front of permanent aircraft features and due partly to the fact that the flow surround the aircraft is highly turbulent causing wake effects from small protuberances to be heavily "washed out" at significant distances downstream of the protuberance.

To fully correlate the wind tunnel data with drag coefficients expected for the full-scale aircraft, a device representing a typical protuberance has been fashioned and attached to the front hatch location. An instrumented full-scale version of this device will be flown on a full-scale aircraft so that the drag coefficient can be determined for the full-scale device at the full-scale Reynolds number. At that point, the wind tunnel data can be correlated to the full-scale drag coefficients by comparing the flight test data with the front hatch measurements in the wind tunnel.

It should be noted that most of the protuberances investigated during the effort described herein experience loading primarily in the axial direction and are instrumented in that direction only. There are some cases in which the aerodynamic load has two significant components and still other cases in which the area in which a protuberance is mounted would experience a significant drag force even if the protuberance were not present. For example, the cockpit roof of the modified C-130 has several protuberances affixed to it. The cockpit roof experiences a drag force without the protuberances affixed. To determine the contribution of the protuberances to drag in this case, the skin of the cockpit roof is instrumented and measurements are taken with the protuberances in place and with the protuberances removed. The difference between these measurements is taken to be the drag induced by the protuberances. In this case, the difference between the measurements is of a similar magnitude to the measurements so that the error associated with subtracting two large numbers to obtain a small drag measurement is avoided.

Model Fabrication

The skin for the wind tunnel model came from a 1/48 scale ***Italeri***™ model kit. Significant effort was expended in checking the dimensional accuracy of the skin and no significant deviations from the full-scale H model C-130 were found. To construct the model from the kit, dramatic structural modifications were required. A tube suitable for mounting the model to the wind tunnel sting balance forms the principle structural support for the model. Hard machined wing and tail structure components are attached to this basic member and bulkheads are custom fitted to allow the skin to be accurately affixed to the underlying structure. The bulkheads are arranged so that the airplane is at zero angle of attack when the sting mount is horizontal.

Before the skin is affixed to the structure, sensor locations are identified and tubes for carrying signals to and from the sensors are installed. A photo showing this structure just before the skin installation is shown in Figure 1.

Once the structure is complete, the skin is installed and the void between the structure and the skin is filled with epoxy. This allows for a rigid structure that will withstand the wind tunnel loading. The holes for the sensors are then machined and the sensors and wiring are installed. A photograph of the completed model in the wind tunnel is shown in Figure 2.

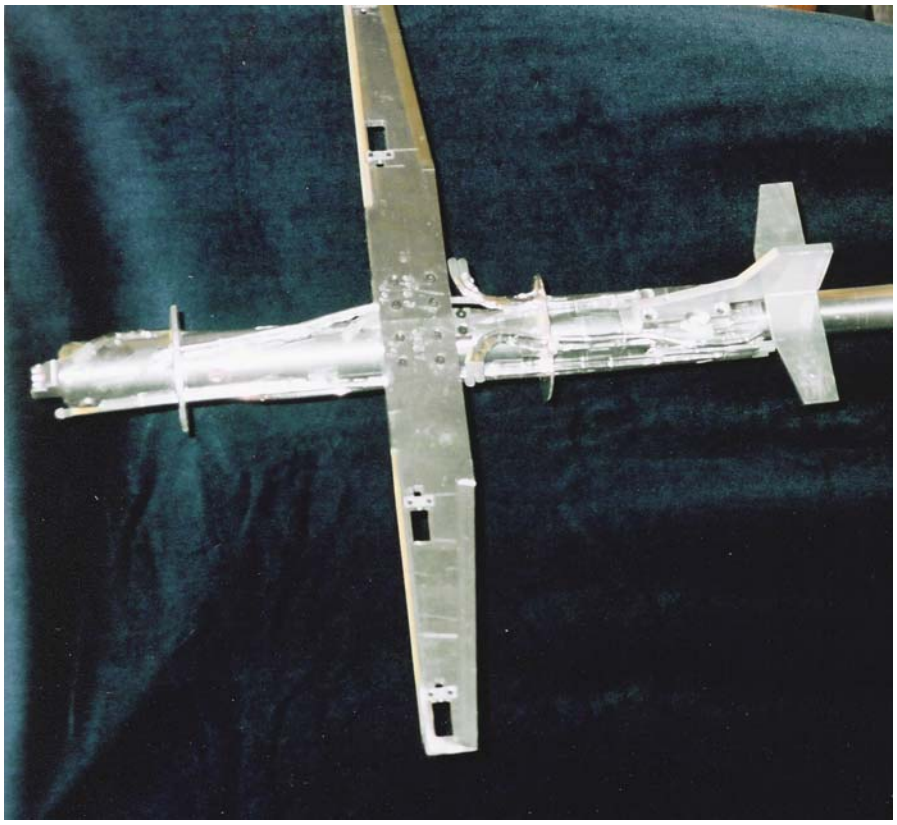

Figure 1: Basic structure of aircraft model with bulkheads installed.

Figure 2: C-130 Model in Wind Tunnel

The sensors used to measure the drag force on each protuberance are constructed using strain gage technology. The protuberances are mounted on the ends of the sensors and are physically separated from the by aircraft model except for the sensor mount. A fuselage protuberance is shown in the photograph in Figure 3 and a wing pylon mounted on a sensor is shown in Figure 4.

Figure 3: Fuselage-mounted protuberance

Figure 4: Wing Pylon mounted on a sensor

Sample Results

Some samples of the results obtained from this effort are shown in Figures 5-11. The data shown in Figure 5 represents the axial force coefficient measured for the outboard pylon with no protrusion mounted on it as a function of angle of attack. (One count is 1/10.000th) and is based on the reference area and ambient conditions for the aircraft or model.) Clearly the axial force coefficient in this case is a strong function of the angle of attack and cannot be treated as a constant for arbitrary flight conditions.

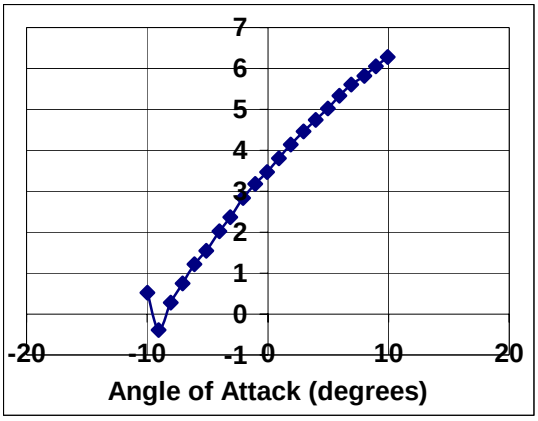

Figure 5: Left Side Outboard Pylon Axial Force Coefficient (Counts)

The data shown in Figure 6 shows a similar trend for the case in which the fuel tank is added to an inboard pylon but with a significantly higher coefficient based on the increased size of the protuberance relative to the aircraft reference area.

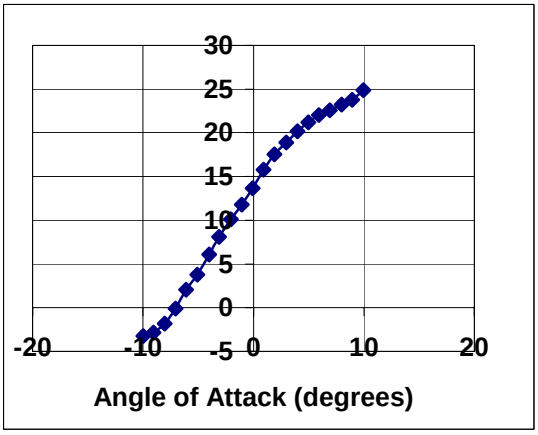

Figure 6: Right Side Inboard Pylon Axial Force Coefficient (counts) (Fuel Tank Attached)

The data shown in Figure 7 is the drag data for the device depicted in Figure 3. This device was constructed for the specific purpose of calibrating the measurements in the tunnel to drag expected to be induced on the aircraft by protuberances. A full scale version of this device can be instrumented and mounted on the full-scale aircraft. Data from the flight test can then be

compared to data from the wind tunnel for the same (scaled) device. Any differences between the two measurements will be due to Reynolds number effects and can be used to adjust the wind tunnel drag coefficient data for the remainder of the protuberances. Clearly, the drag coefficient for this protuberance is a function of angle of attack but the dependence on angle of attack is relatively small (approximately 10% over the entire angle of attack range) and this variation is expected to be small on the full scale aircraft.

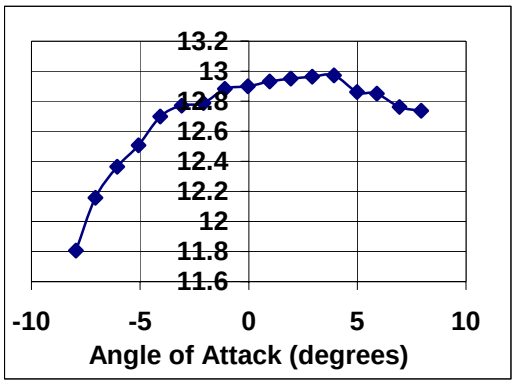

Figure 7: Front Hatch Protuberance Axial Force Coefficient (counts)

The data shown in Figure 8 is from a protuberance mounted directly behind the wing. This data is included here simply to illustrate how the downwash from the wing or from another protuberance can affect the drag on a protuberance. In this case, the wing is directly in front of this protuberance at an angle of attack of approximately -5°. The drag coefficient measured based on free stream conditions clearly dips in this region because the local flow velocity is substantially reduced by the presence of the wing.

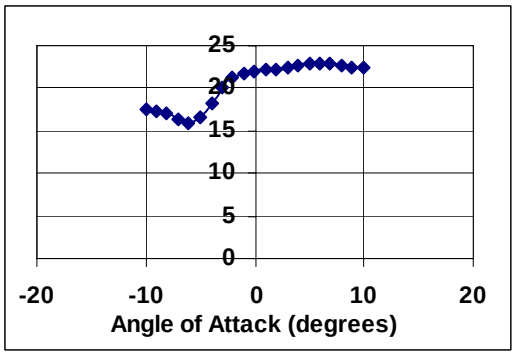

Figure 8: Protuberance mounted behind the wing (Counts)

The data shown in figures 9, 10 and 11 illustrate the method used to obtain drag data for devices mounted on surfaces which are not nearly parallel to the free stream flow direction. For the C-130 model tested, some devices are located on the cockpit roof and this area will obviously see a significant axial force even in the absence of protuberances. To access the drag induced by the protuberances only, data for this skin area was collected with the protuberances attached and without the protuberances attached. The difference between these two data sets represents the drag induced by the protuberances. The data shown in figure 9 for the case in which the protuberances are attached, is somewhat eratic as one might expect from a aerodynamically cluttered environment such as the one formed by the cockpit roof with protuberances.

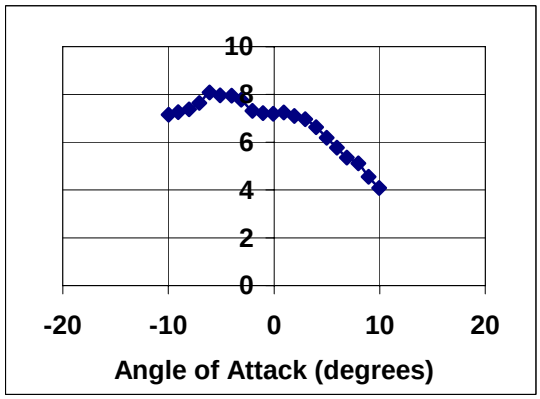

Figure 9: Cockpit Roof With Devices Attached (Counts)

The data shown in Figure 10 is indicative of a smooth or clean aerodynamic environment and is generally significantly lower as expected. It should be pointed out that the data in Figures 9 and 10 does not represent the drag associated with the section of cockpit roof instrumented; however, the difference between the data shown in Figure 9 and the data shown in figure 10 does represent, to a high degree of approximation, the increase in aircraft drag due to the presence of the protuberances.

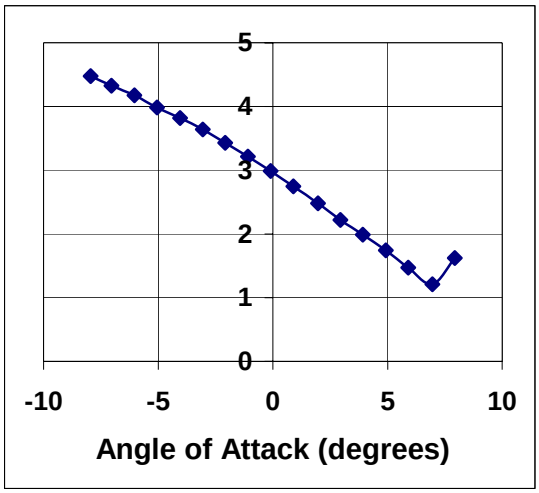

Figure 10: Cockpit Roof Without Protuberances (Counts)

This calculation is represented in Figure 11. Clearly the protuberances add significantly to total aircraft drag, however, the strong dependence on angle of attack is not exhibited in this data as it is in the data for other protuberances discussed earlier. This is due at least partly to the fact that the flow conditions near this area of the fuselage do not change significantly with angle of attack.

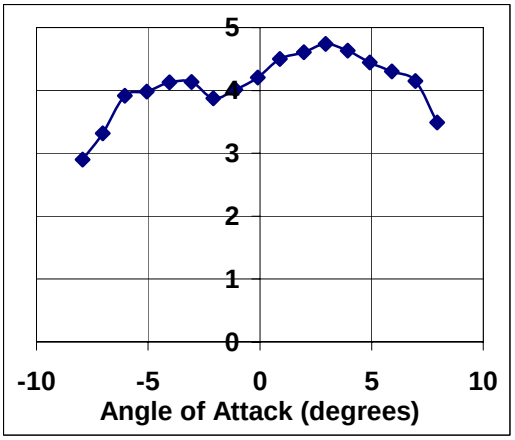

Figure 11: Drag due to Cockpit Roof Protuberances

Measurement Error

In any experimental measurement including wind tunnel testing, both systematic and statistical errors in the measurement are always a concern. In the present test, the uniqueness of the sensor arrangement and the very small drag loads for each sensor posed a special problem in eliminating systematic errors. Each sensor output resulted from a full bridge (resistance bridge) coming from strain gages that were 1/16 th inch in length. The sensor itself was designed to measure maximum loads that were on the order of 0.3 pounds force. The resulting mechanism was very delicate and may have contributed to some errors in the results.

Additionally, systematic errors may result from small changes in the applied voltage to the bridge circuits. Although this was checked frequently during the tests, minor changes could have influenced the resulting data. Fundamentally, measurement error always occurs when samples of a given quantity are queried. These statistical errors are generally very small for measurements with large dynamic range as exists in the signal conditioning and data acquisition used in this study. To gain further confidence that the

statistical error is low, some of the data was repeated with essentially the same results as previous runs. The data appears to be self-consistent in that measurements axial force coefficients for symmetric devices collected independently on each side of the fuselage produced practically identical results.

Conclusions and Recommendations

There are some general conclusions that can be made from an analysis of the data as presented in Figs 5-11, but not all of the behavior exhibited by the drag measurements can be readily explained with confidence without further in-stream measurement of flow properties.

First, it is critically important that recognition be given to the fact that the drag coefficients for the protuberances are generally dependent on angle of attack. In some cases, this dependence is very strong (under wing protuberances) and in other cases the dependence is weak. Nevertheless, one cannot simply choose a number for the drag counts induced by a given protuberance and expect to obtain accurate predictions of the drag for the protuberance for all flight conditions using that single number.

Secondly, it should be noted that the sum of all of the drag increments on any one run, signify the total drag for the protuberances collectively. However, one cannot simply add up the protuberance drag counts and get the total drag increment due to the protuberances in any general case. The drag count as measured on an individual protuberance does not account for *interference* drag. Part of the drag associated with a protuberance is associated with the fact that the protuberance is *attached* to the aircraft. This is analogous to the lift produced by a wing. If it is isolated, a wing will produce a given amount of lift. If attached to an airplane under the same conditions (Mach number, Reynolds number, angle of attack, and etc) it will produce a different lift. The same is true for protuberance drag components. The sensors only measure the net aerodynamic axial force produced on the sensor directly. There is an additional component of drag induced on the aircraft because the protuberance is attached. This is small in most cases and the protuberances on the aircraft tested are configured in such a way that the interference and induced drag are likely to be less than the interference and induced drag aircraft with other configurations. The main balance data accounts for *all* the drag but, of course, is much less sensitive.

References:

1. Rae, William H. and Pope, Alan, Low-Speed Wind Tunnel Testing, Second Edition, John Wiley and Sons, Toronto, 1984.
2. Taylor, John R., An Introduction to Error Analysis, University Science Books, Oxford University Press, Mill Valley CA, 1982.
3. Schlichting, Hermann, Boundary-Layer Theory, McGraw-Hill, New York, 1979.